

Johari-Goldstein secondary relaxation in methylated alkanes

K. L. Ngai

Naval Research Laboratory, Washington, DC 20375-5320, USA

(Received 2 December 2004; revised manuscript received 17 February 2005; published 17 June 2005)

Dielectric relaxation measurements of the methylated alkanes, 3-methylpentane, 3-methylheptane, 4-methylheptane, 2,3-dimethylpentane, and 2,4,6-trimethylheptane by S. Shahriari, A. Mandanici, L-M Wang, and R. Richert [J. Chem. Phys. **121**, 8960 (2004)] have found a primary α relaxation of these glass-forming liquids and a slow secondary β relaxation that are in close proximity to each other on the frequency scale. These glass formers have one or more methyl groups individually attached to various carbons on the alkane chain. They cannot contribute to such a slow secondary relaxation. Hence the observed secondary relaxations is not intramolecular in origin and, similar to secondary relaxations found in rigid molecules by Johari and Goldstein, they are potentially important in the consideration of a mechanism for the glass transition. These secondary relaxations in the methylated alkanes are special and belong to the class of Johari-Goldstein in a generalized sense. The coupling model has predicted that its primitive relaxation time should be approximately the same as the relaxation time of the secondary relaxation if the latter is of the Johari-Goldstein kind. This prediction has been shown to hold in many other glass formers. The published data of the methylated alkanes provide an opportunity to test this prediction once more. The results of this work confirm the prediction.

DOI: 10.1103/PhysRevB.71.214201

PACS number(s): 64.70.Pf, 77.22.Gm, 65.20.+w

I. INTRODUCTION

Some secondary relaxations bear no relation in dynamic properties with the primary or α relaxation. An example is the lack of any appreciable pressure dependence of the secondary relaxation time in contrast to the observed strong pressure dependence of the α relaxation in many glass formers.¹⁻⁴ These secondary relaxations likely have intramolecular origin, involving local motion of a part of the molecule, and are unimportant for the consideration of glass transition. On the other hand, there is a restricted class of secondary relaxations having properties that mimic the α relaxation. Notable examples include⁴ (1) a significant pressure dependence and a non-Arrhenius temperature dependence of its relaxation time in the equilibrium liquid state, (2) a change in slope of the temperature dependence of its dielectric strength when crossing the glass transition temperature T_g in a manner similar to the specific volume, enthalpy, and entropy, (3) a good correspondence⁵⁻⁹ between the its relaxation time and the primitive relaxation time of the coupling model.¹⁰⁻¹³ The existence of this special class of secondary relaxations was first suggested by the discovery of secondary relaxation in totally rigid molecules by Johari and Goldstein.¹⁴⁻¹⁷ Since rigid molecules have no internal degree of freedom, their secondary relaxation cannot be assigned to any trivial motion of an internal part of the molecule. It must involve motion of the molecule as a whole, thereby acting naturally as the precursor of the “cooperative” many-molecule α relaxation. The secondary relaxation of rigid molecules share the properties of the special class of secondary relaxations in nonrigid glass-formers, which are not intramolecular in origin. In honor of the important discovery by Johari and Goldstein, it is appropriate to use the term JG relaxation to stand for this special kind of secondary relaxations in rigid as well as in some nonrigid glass formers. On the other hand, the purpose or intention is ambiguous when indiscriminately any observed secondary relaxation is called

a JG relaxation without applying any criterion.

There are indications that the JG relaxation is universal, present in all glass formers. It is most familiar in small molecular and polymeric glass formers. The JG relaxation has weaker relaxation strength than the α relaxation, and in some cases may not be resolved when it is not well separated from the α relaxation in time/frequency scale. Nevertheless, it has been found even in other classes of materials where its occurrence is somewhat a surprise. Examples include the molten salt $0.4\text{Ca}(\text{NO}_3)_2\text{-}0.6\text{KNO}_3$ (CKN),¹⁸ the plastic crystals^{19,20} especially the rigid ones such as cyanoadamantane and the metallic glasses.²¹

Most recently, secondary relaxations were found even in some simple glass-forming methylated alkanes including 3-methylpentane, 3-methylheptane, 4-methylheptane, 2,3-dimethylpentane, and 2,4,6-trimethylheptane by Richert and co-workers.²² Reference 22 called these substances branched alkanes, but the word “branched” may give the wrong impression of the presence of long side chains. For this reason, we prefer to describe them here as methylated alkanes. Except for the methyl groups, which execute fast rotations, there are no side groups in these methylated alkanes that can account for the slow secondary relaxations observed. Thus they are likely secondary relaxations of the JG kind. In this work the dielectric spectra of these methylated alkanes are analyzed according to the coupling model description of the evolution of dynamics from the primitive/independent relaxation to the cooperative many-molecule α relaxation, and from which the primitive relaxation times are calculated. The calculated primitive relaxation times are found to be in good correspondence with the relaxation times of the observed secondary relaxations, as previously found for JG relaxations in many other glass formers.⁴⁻⁹

The methylated alkanes are basically hydrocarbons. Hence, the results of this work are compared with the JG relaxation and the α relaxation associated with a

polyethylene-like glass transition occurring within the self-assembled alkyl nanodomains with a typical size of 0.5–2 nm formed by the aggregation of alkyl groups of different monmeric units of higher poly(*n*-alkyl acrylates) and poly(*n*-alkyl methacrylates) in the melt.^{23,24}

II. COUPLING MODEL INTERPRETATION OF α - AND JG RELAXATION

The coupling model (CM) emphasizes the many-body nature of the α -relaxation dynamics of a neat glass former through the intermolecular coupling of the relaxing species with others in its environment.^{10–13} A rigorous solution of simple coupled system^{10,11} has given support to the premise of the CM. Here we restate in brief the physical basis of the CM before extending it to include the connection to the JG relaxations. The many-molecule α dynamics are heterogeneous²⁵ and complicated and only averages over these heterogeneities are considered in the CM. The CM recognizes that all attempts of relaxation have the same primitive rate τ_0^{-1} , but the many-body or many-molecule dynamics prevent all attempts of molecules to be simultaneously successful, resulting in faster and slower relaxing molecules or heterogeneous dynamics. However, when averaged, the effect is equivalent to the slowing down of τ_0^{-1} by another multiplicative factor, which is time dependent. The time-dependent rate $W(t)$ has the product form $\tau_0^{-1}f(t)$, where $f(t) < 1$. In particular, it has to be

$$W(t) = \tau_0^{-1}(\omega_c t)^{-n} \quad (1)$$

with $0 \leq n < 1$, in order that the solution of the averaged correlation function ϕ from the rate equation $d\phi/dt = -W(t)\phi$, is the empirical Kohlrausch stretched exponential function

$$\phi(t) = \exp[-(t/\tau_\alpha)^{1-n}]. \quad (2)$$

Here n is the coupling parameter of the CM and $\beta \equiv (1-n)$ is the fractional Kohlrausch exponent. More important the many-molecule dynamics or the extent of the dynamic heterogeneity, larger is the coupling parameter n and vice versa. The time-dependent rate $\tau_0^{-1}(\omega_c t)^{-n}$ also leads immediately to the most important relation between τ_α and τ_0 of the CM given by

$$\tau_\alpha = (t_c^{-n} \tau_0)^{1/(1-n)}, \quad (3)$$

after identifying t_c introduced here by $t_c = (1-n)^{-1/n} / \omega_c$. Many-molecule dynamics cannot start instantly. In fact, from neutron-scattering experiments and molecular dynamics simulations of polymeric and small molecular liquids performed at short times,¹³ the Kohlrausch function no longer holds at times shorter than approximately 2×10^{-12} s, and is replaced by the linear exponential time dependence of the primitive relaxation. This property indicates that t_c is approximately equal to 2 ps for small molecule and polymeric glass formers.¹³

The CM described above has recently been extended to make the connection of its primitive relaxation time τ_0 with the most probable relaxation time of the Johari-Goldstein

relaxation.^{4–9,26} Such a connection is expected from the similar characteristics of the two relaxation processes⁴ including (1) their local nature and (2) involvement of the entire molecule, and acting as the precursor of the α relaxation.

Since it may seem that there is now another role played by the primitive relaxation, *separate* and *distinctive* from that described in the above for the Kohlrausch α relaxation, it is necessary to give the following clarifications. At short times, when there are few independent relaxations present, they appear separately in space as localized motions just as with the JG relaxation. Hence

$$\tau_{JG}(T) \approx \tau_0(T), \quad (4)$$

and this is one role played by the independent relaxation. At times beyond τ_0 or τ_{JG} , more units can independently relax, but they cannot be considered as isolated events anymore, because some degree of cooperativity (or dynamic heterogeneity) is required for the motions to be possible. The degree of cooperativity and the corresponding length scale continues to increase with time as more and more units participate in the motion, as suggested by the evolution of dynamics of colloidal particles with time obtained by confocal microscopy.²⁷ These time evolving processes contribute to the JG relaxation at time longer than τ_0 or τ_{JG} over an extended time range until the maximum cooperative (or dynamic heterogeneity) length scale is reached. From then on, the α relaxation having the averaged correlation function of Kohlrausch takes over. This description of the evolving dynamics means that the JG relaxation are responsible for a broad dispersion, similar in spirit to a Cole-Cole or Havriliak-Negami distributions customarily assumed to represent the JG relaxation in the literature by many workers. Within this definition of the JG relaxation, experiment performed to probe it will find that “essentially” all molecules contribute to the JG relaxation and the motions are dynamically and spatially heterogeneous as found by dielectric hole burning²⁸ and deuteron NMR (Ref. 29) experiments. This coupling model description of the JG relaxation may help to resolve the different points of view on its nature between Johari¹⁷ and others.^{28–33}

The *fully* cooperative (or dynamic heterogeneous) α -relaxation regime has the maximum cooperative volume or dynamic heterogeneity length scale L_{DH} at the given temperature. The averaged correlation function of the fully cooperative α relaxation has the fractional exponential Kohlrausch form of Eq. (2). The extent of heterogeneous dynamics is L_{DH} , and the deviation of the Kohlrausch function from linear exponential is measured by n . Both heterogeneous dynamics and of Kohlrausch are both parallel consequences of the slowing down of the primitive relaxation by many-molecule dynamics. Therefore, naturally a larger L_{DH} is associated with a larger coupling parameter n appearing in the fractional exponent $(1-n)$ of the Kohlrausch function because both are measures of the many-molecule dynamics. Broad-band dielectric relaxation measurements found in some glass-formers that the dispersion of the α relaxation narrows and hence n decreases with decreasing τ_α on increasing temperature above T_g . The correlation between L_{DH} and n from the CM implies in anyone of these glass formers

that L_{DH} follows n to decrease with decreasing τ_α on increasing temperature. On the other hand, for some glass-formers such as $\alpha\alpha\beta$ -tris-naphthylbenzene,³⁴ which has a constant n over a considerable temperature range above T_g , the CM would predict that L_{DH} is constant over the same temperature range. In general, comparisons of the parameters L_{DH} and n of different glass formers should be made uniformly at constant τ_α , preferably all at their respective T_g 's where τ_α is equal to a long time and n is no longer temperature dependent. The more stringent test of the correlation is on glass formers of the same class, such as sorbitol, xylitol, threitol, and glycerol. Although not the ideal test of glass formers in the same class, the correlation between L_{DH} and n is borne out by comparing L_{DH} for glycerol, ortho-terphenyl, and poly(vinylacetate) obtained by multidimensional ^{13}C solid-state exchange NMR experiments.^{35–37} These experiments found, at about $T=T_g+10$ K, the number of molecules per slow domain is 390 monomer units for poly(vinylacetate), 76 molecules for ortho-terphenyl, and only 10 molecules for glycerol. The coupling parameter n deduced from the Kohlrausch fit to the dielectric spectra near $T=T_g$ is 0.53, 0.50, and 0.29 for poly(vinylacetate),³⁸ ortho-terphenyl,³⁹ and glycerol^{6,40} respectively. NMR experiments also confirm that the distribution of relaxation rates is narrower for glycerol than it is for either poly(vinylacetate) or ortho-terphenyl.³⁷

There is a further experimental evidence of the close connection between the primitive relaxation and the JG relaxation from the size of their jump angles. In the context of the CM described above, the primitive relaxation is the underlying mechanism of the dynamically heterogeneous molecular reorientations of the α relaxation. Thus, characteristics of the primitive relaxation can be deduced from the dynamically heterogeneous molecular reorientation of the α relaxation. Multidimensional NMR^{32,33} experiments have shown that the dynamically heterogeneous molecular reorientations of α relaxation occurs by relatively small jump angles with exponential time dependence, just like that of the primitive relaxation. Furthermore, from one and two-dimensional ^2H NMR studies,^{30,31} the JG relaxation in toluene- d_5 and polybutadiene- d_6 also involves small angle jumps of similar magnitude at temperatures above T_g . This similarity in size of the jump angles of the primitive relaxation and the JG relaxation again supports the connection between these two relaxation processes. They give rise to the dynamically heterogeneous α relaxation through the many-molecule dynamics.

III. COUPLING MODEL ANALYSIS OF α - AND JG RELAXATION IN METHYLATED ALKANES

Richert and co-workers²² have used an ultraprecision capacitance bridge to make possible the dielectric relaxation measurements of several glass-forming methylated alkanes with very low dielectric loss in the frequency range 50 Hz to 20 kHz. The molecular liquids of this study are 3-methylpentane, 3-methylheptane, 4-methylheptane, 2,3-dimethylpentane, and 2,4,6-trimethylheptane. All liquids display asymmetric α -loss peaks typical of supercooled liquids and secondary β relaxations of smaller amplitudes. We here

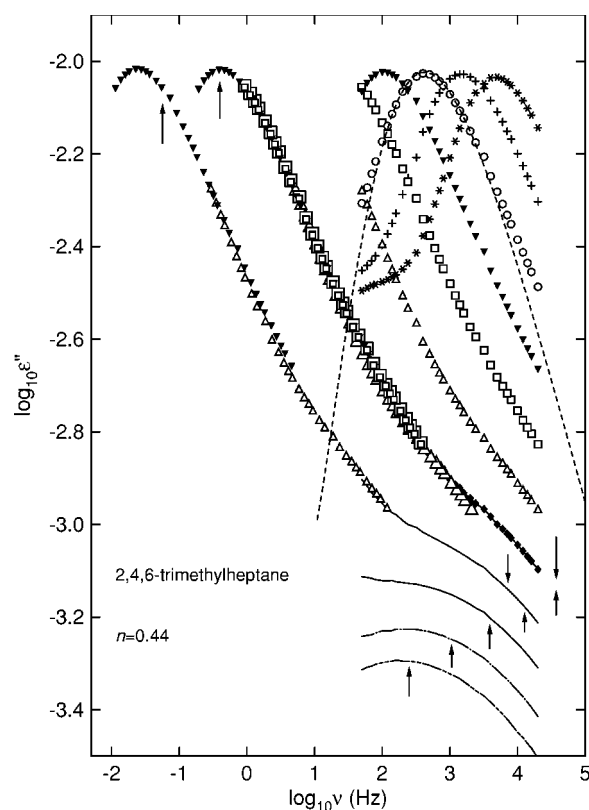


FIG. 1. Dielectric loss $\epsilon''(\nu)$ versus logarithmic frequency for 2,4,6-trimethylheptane. The actually measured loss data all lie within the limited frequency range 50 Hz to 20 kHz. The isothermal data in this frequency range in descending order were taken at 140, 138, 136, 134, 132, 130, 128, 126, 124, 122, and 120 K. Some of the lower-temperature data are shown as lines. The dashed line is the KWW fit to the data at 136 K with $n=0.44$. For explanation of the two master curves constructed by time-temperature superposition of isothermal loss data, and the legends of the arrows, see text.

analyze their results with the coupling model (Sec. II). The fit to the dielectric loss peak in the isothermal loss data by the one-sided Fourier transform of the Kohlrausch function [Eq. (2)] determines the two parameters, n and τ_α , characterizing the α relaxation at that temperature. The primitive relaxation times τ_0 are calculated from these α -relaxation parameters via Eq. (3), and compared with the observed secondary relaxation time of each of the methylated alkanes. The purpose of the exercise is to check whether the coupling model prediction for JG relaxation, Eq. (4), holds for the methylated alkanes or not.

A. 2,4,6-trimethylheptane (246TMH)

This is the largest molecule of the methylated alkanes studied. In Fig. 1 the actually measured loss data lie within the limited frequency range 50 Hz to 20 kHz of the ultraprecision capacitance bridge. In this frequency range the four loss peaks at $T=140, 138, 136,$ and 134 K have the same shape and can all be fit with the Kohlrausch-Williams-Watts function, i.e., the one-sided Fourier transform of the Kohlrausch function [Eq. (2)], with $n=0.44$. An example of the fit

to the data at 136 K is shown by the dashed line in Fig. 1. In fitting the α loss by the Kohlrausch function, emphasis is placed in obtaining good fit to the data near the peak and its low frequency flank assuming there is no significant contribution from conductivity or impurities. Inevitably, the Kohlrausch fit underestimates the loss on the high frequency flank of the α loss. According to the CM description of the evolution of molecular dynamics with time (Sec. II), this endemic deviation on the high-frequency flank is attributed to the developing cooperative processes with increasing length scale that occurs in between the primitive relaxation and the fully cooperative α relaxation having the Kohlrausch form. The other isothermal data in the same frequency range in descending order were taken at 132, 130, 128, 126, 124, 122, and 120 K. The secondary relaxation is clearly resolved as shoulders or peaks at the lower temperatures. For two of these lower temperatures, 128 and 126 K, we constructing master curves to extend the range to lower frequencies. Each master curve shown in Fig. 1 is obtained by shifting the actual data taken at higher temperatures horizontally to superpose onto each other. A small vertical shift is applied to account for the change in loss peak height according to the $(1/T)$ dependence, which has been established from the actual data taken at higher temperatures. The loss peak frequencies of the master curves are approximately the frequencies of the α peak ν_α at 128 and 126 K. Another estimate of ν_α can be obtained from the fit to the Vogel-Fulcher-Tammann (VFT) law

$$\log_{10}(\tau_\alpha/s) = A + B/(T - T_0) \quad (5)$$

given in Ref. 22 with $A = -18$, $B = 778$ K, and $T_0 = 83.8$ K. This estimate of ν_α are shown by an upward pointing vertical arrow near the α peak of the master curve at 128 and 126 K, respectively. There is good correspondence between the two approximations to ν_α . The primitive frequency, ν_0 , calculated by a variant of the CM equation (3),

$$\nu_0 = (\nu_c)^n (\nu_\alpha)^{1-n}, \quad (6)$$

where $n = 0.44$, $\nu_c = 79.6$ GHz (corresponding to $t_c = 2$ ps), is shown for each temperature by the vertical arrows. The downward pointing arrows indicate ν_0 calculated from ν_α determined as the loss peak frequency of the master curves at 128 and 126 K. The upward pointing arrows in the secondary relaxation region indicate ν_0 calculated from ν_α obtained by the VFT law [Eq. (5)] for all five temperatures 128, 126, 124, 122, and 120 K. The locations of the vertical arrows are near where one would identify as the characteristic frequencies of the secondary relaxation ν_β . We can conclude that the calculated ν_0 agrees well with ν_β and hence Eq. (4) is valid. The results support the conclusion that the observed secondary relaxation in 2,4,6-trimethylheptane is a JG relaxation.

At the lowest temperature 120 K of data shown in Fig. 1, $\tau_\alpha = 10^{3.5}$ s, which is quite long and this value obtained by extrapolating the VFT equation may no longer be a good estimate. An Arrhenius temperature dependence replaces the VFT dependence in the glassy state, and thus the actual τ_α at 120 K may be shorter than $10^{3.5}$ s. This overestimate of τ_α at 120 K may have something to do with the discrepancy that the well-resolved secondary (JG) loss process at 120 and

122 K have nearly the same peak frequency, while the calculated ν_0 at these two temperatures differ by about 0.6 of a decade (Fig. 1).

In Fig. 1, the master loss curves at 126 and 128 K constructed by shifting data at higher temperatures give a false impression of the presence of an additional excess wing (i.e., a second weaker power law at the high-frequency flank of the α -loss peak before reaching the JG relaxation). This feature is an artifact of the shifting procedure and in fact it originates from the data taken at the higher temperature of 128 K (open triangles). At 128 K and temperatures above, ν_β is not much higher than ν_α , and the JG relaxation is not resolved and shows up as excess wing at the higher temperatures. The true low-temperature curves (if measured) would not have an excess wing and thus the master curves should not be shifted to low frequencies as far as indicated in Fig. 1, which may also explain the discrepancy between the peak frequencies of the master curve and that obtained by the VFT equation (vertical arrow) at 126 K. Similar remarks apply to other figures to be introduced in the subsections to follow.

The procedure used to extract the parameters n and ν_α and the construction of the master loss curves at lower temperatures for 246TMH are repeated for the other methylated alkanes. For the sake of brevity, they are not duplicated in the following subsections. Only brief description of the data of the other methylated alkanes are given here. The details can be found in Ref. 22.

B. 3-methylpentane (3MP)

The fits to the actually measured loss data of 3-methylpentane in the frequency range 50 Hz to 20 kHz by the Kohlrausch-Williams-Watts (KWW) function all yield $n = 0.39$. An example is shown by the dashed curve for one of the isothermal loss data in Fig. 2. The spectra in ascending order were taken from 78 to 96 K with an increase of 2 K for consecutive ones. The secondary relaxation is resolved as a shoulder or peak at lower temperatures. The master curve constructed for the two lower temperatures show the entire dispersion. There is good correspondence between the ν_α determined as the loss peak frequency of the master curves and from the VFT law given in Ref. 22. The legends of the arrows drawn are the same as in Fig. 1. The primitive frequencies ν_0 calculated by Eq. (6) with ν_α taken as the peak frequency of the master curves are shown by the downward pointing arrows. The upward pointing arrows in the secondary relaxation region indicate ν_0 calculated from ν_α obtained by the VFT law of 3-methylpentane given in Ref. 22. The calculated ν_0 are in agreement with ν_β and hence we conclude that the observed secondary relaxation in 3-methylheptane is a JG relaxation.

The intensity of the β relaxation relative to that of the α relaxation as well the separation between their frequencies of 3-methylpentane at constant ν_α are remarkably similar to 1,1'-di(4-methoxy-5-methylphenyl)cyclohexane (BMMPC) (Ref. 41) and iso-amyl bromide,⁴² in spite of the much larger dipole moment of these two other glass formers. BMMPC and iso-amyl bromide have values of n equal to 0.40 and 0.39 respectively, practically the same as that of

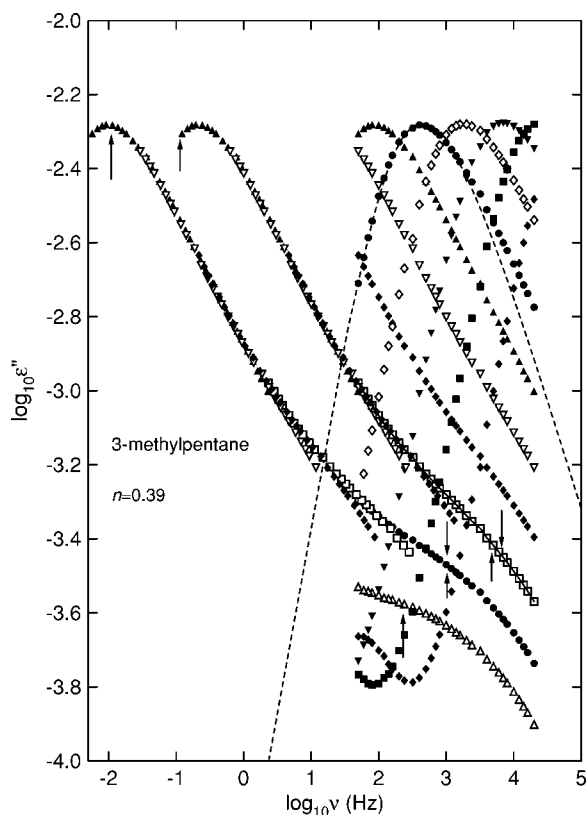


FIG. 2. Dielectric loss $\varepsilon''(\nu)$ versus logarithmic frequency for 3-methylpentane (Ref. 22). The actually measured loss data all lie within the limited frequency range 50 Hz to 20 kHz. The spectra in ascending order were taken from 78 to 96 K with an increase of 2 K for consecutive ones. The dashed line is the KWW fit to the one set of data with $n=0.39$. For explanation of the two master curves constructed and the legends of the arrows, see text.

3-methylpentane. The three structurally very different glass formers, 3-methylpentane, BMMPC and iso-amyl bromide, is an example that the coupling parameter n or the Kohlrausch exponent $(1-n)$ of the α -relaxation principally determines the relation of the JG relaxation to the α relaxation. Qualitatively, this can be expected from the Coupling Model description in Sec. II of the evolution of molecular dynamics as a function of time from the primitive relaxation (or the JG relaxation) to the α relaxation. In this description, the increasingly cooperative processes with developing length scale that occurs in between the primitive relaxation and the α relaxation are similar if n is the same independent of the glass former, as long as τ_α or equivalently τ_0 [Eq. (3)] is kept constant. Thus the dielectric spectra of different glass-formers having the same n become approximately isomorphic after normalization by the maximum loss of the α relaxation. For comparison of normalized spectra of glass formers with different n , see Fig. 12 in Ref. 43.

C. 2,3-dimethylpentane (23DMP)

The fits to the actually measured loss data of 2,3-dimethylpentane in the frequency range 50 Hz to 20 kHz by the KWW function all yield $n=0.39$, same as

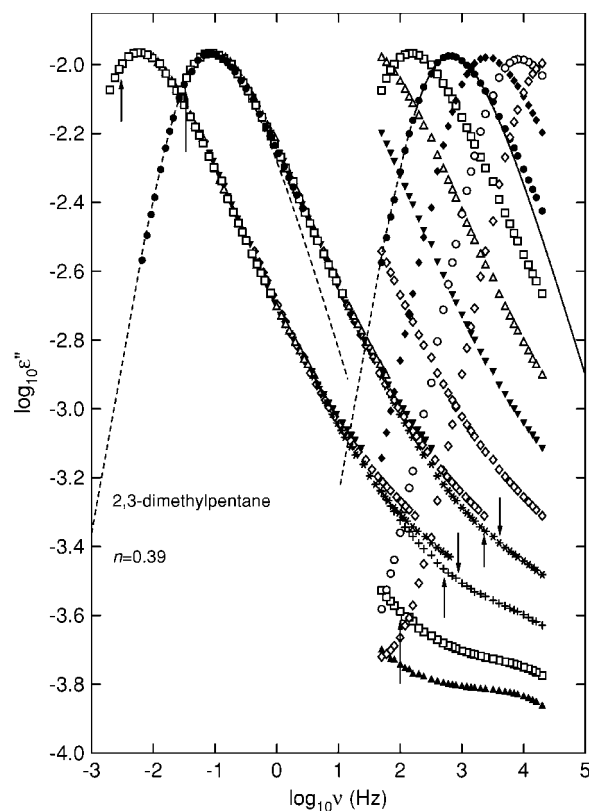


FIG. 3. Dielectric loss $\varepsilon''(\nu)$ versus logarithmic frequency for 2,3-dimethylpentane (Ref. 22). The actually measured loss data all lie within the limited frequency range 50 Hz to 20 kHz. The spectra in ascending order were taken from 84 to 104 K with an increase of 2 K for consecutive ones. The dashed line is the KWW fit to the one set of data with $n=0.39$. For explanation of the two master curves constructed and the legends of the arrows, see text.

3-methylpentane. An example is shown by the solid curve in Fig. 3. The spectra in ascending order were taken from 84 to 104 K with an increase of 2 K for consecutive ones. However, the intensity of the secondary relaxation relative to that of the maximum α loss is smaller in 2,3-dimethylpentane than in 3-methylpentane. This difference possibly explains the secondary relaxation in 2,3-dimethylpentane was observed mainly as a shoulder, while in 3-methylpentane it is more pronounced (Fig. 2). The master curves in Fig. 3 also bear resemblance to BMMPC and iso-amyl bromide in dispersion. The legends for the arrows in Fig. 3 are the same as in Figs. 1 and 2. The lowest temperature for which ν_0 is calculated is 86 K, where VFT equation indicates that $\tau_\alpha=10^{2.9}$ s. Calculated ν_0 at 84 K is not reported because the VFT value of $\tau_\alpha=10^{4.2}$ s is no longer reliable. There is large uncertainty in the location of ν_β because of secondary relaxation shows up as a broad shoulder. Nevertheless the calculated ν_0 can be considered as a rough indicator of ν_β for 2,3-dimethylpentane.

D. 3-methylheptane (3MH)

The spectra shown in Fig. 4 in ascending order were taken from 98 to 118 K with an increase of 2 K for consecutive

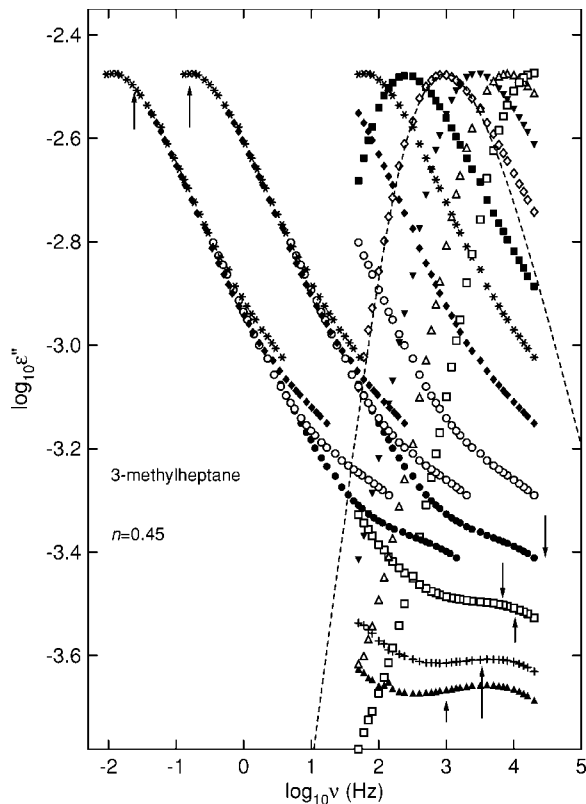


FIG. 4. Dielectric loss $\varepsilon''(\nu)$ versus logarithmic frequency for 3-methylheptane (Ref. 22). The actually measured loss data all lie within the limited frequency range 50 Hz to 20 kHz. The spectra in ascending order were taken from 98 to 118 K with an increase of 2 K for consecutive ones. The dashed line is the KWW fit to the one set of data with $n=0.45$. For explanation of the two master curves constructed and the legends of the arrows, see text.

ones. The KWW fits to the actually measured loss data of 3-methylheptane yield the largest coupling parameter $n=0.45$ among the methylated alkanes studied in Ref. 22 (see Fig. 4 here). This happens possibly because of the location of the methyl group, making the molecule asymmetric and hence increasing the intermolecular constraints between the molecules. In contrast, the symmetric molecule 4-methylheptane has the smallest $n=0.28$ as we shall see in the next subsection.

Similar to 2,4,6-trimethylheptane with a comparable $n=0.44$, the secondary relaxation of 3-methylheptane is well separated from the α -loss peak and shows up as resolved peaks in the isothermal spectra (Fig. 4). The legends for the arrows drawn in Fig. 4 are the same as given in Figs. 1–3. The lowest temperature for which ν_0 is calculated is 96 K, where VFT equation indicates that $\tau_\alpha=10^{2.7}$ s. The calculated ν_0 is in good order of magnitude agreement with the loss peak frequency ν_β of the JG relaxation. Equation (4) is valid and hence the observed secondary relaxation in 3-methylheptane is the JG relaxation.

E. 4-methylheptane (4MH)

The spectra shown in Fig. 5 in ascending order were taken from 98 to 120 K with an increase of 2 K for consecutive

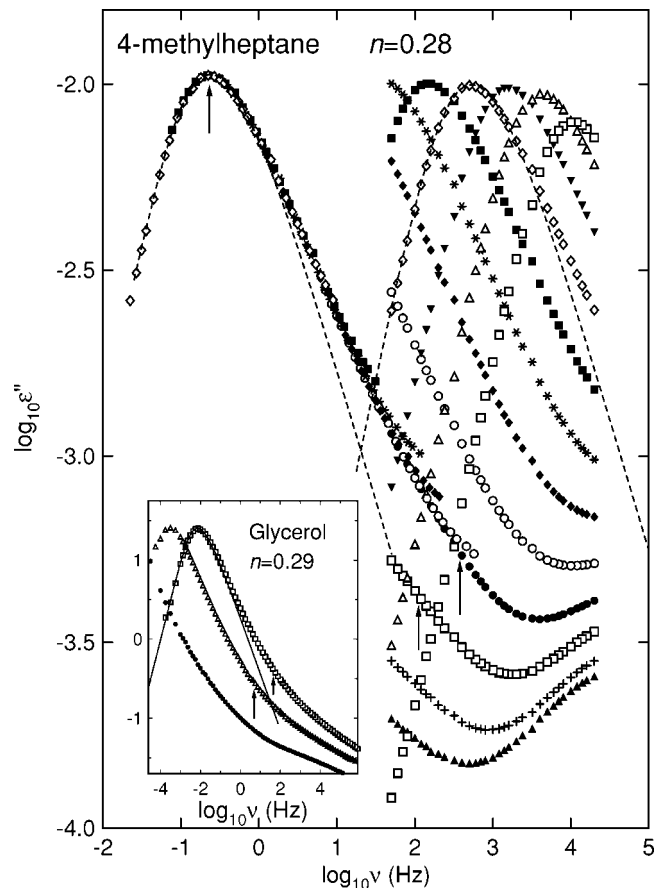


FIG. 5. Dielectric loss $\varepsilon''(\nu)$ versus logarithmic frequency for 4-methylheptane (Ref. 22). The actually measured loss data all lie within the limited frequency range 50 Hz to 20 kHz. The spectra in ascending order were taken from 98 to 120 K with an increase of 2 K for consecutive ones. The dashed line is the KWW fit to the one set of data with $n=0.28$. For explanation of the two master curves constructed and the legends of the arrows, see text. The inset shows the dielectric loss $\varepsilon''(\nu)$ versus logarithmic frequency for glycerol from Ref. 40 together with the KWW fit (Ref. 6) with $n=0.29$.

ones. The α -loss peak of 4-methylheptane is significantly narrower than all the other alkanes discussed before. Naturally, the KWW fits to the actual data of 4-methylheptane in Fig. 5 gives a significantly smaller coupling parameter $n=0.28$. From Eq. (6), the separation between ν_0 and ν_α (in units of Hz) on a logarithmic scale is given by

$$\log_{10} \nu_0 - \log_{10} \nu_\alpha = n(10.9 - \log_{10} \nu_\alpha). \quad (7)$$

Combined with the other CM relation $\nu_0 \approx \nu_{JG}$ [i.e., Eq. (4)], we have

$$\log_{10} \nu_{JG} - \log_{10} \nu_\alpha \approx n(10.9 - \log_{10} \nu_\alpha), \quad (8)$$

which says that the separation between ν_{JG} and ν_α is smaller for a smaller n at constant ν_α . As an example, for 4-methylheptane and $\nu_\alpha=10^{-1}$ Hz, the separation is 3.3 decades from $n=0.28$, compared with 5.36 decades from $n=0.45$ if it is 3-methylheptane. The proximity of the JG relaxation to the dominant α -loss peak makes it difficult for

the former to be resolved from the latter in 4-methylheptane. Thus the JG relaxation in 4-methylheptane is not resolved but hidden on the high frequency flank of the α -loss peak as suggested by the location of the calculated ν_0 for the master curves constructed for the real data at 104 K in the main part of Fig. 5. Since the peak frequency ν_α of the master curve is practically the same as that from the VFT law given in Ref. 22, it is sufficient in Fig. 5 to indicate the calculated ν_0 by a single vertical arrow. The other vertical arrow nearby indicates the calculated ν_0 for the data taken at 102 K. In Fig. 5 in the experimental spectra of 4MH at 98, 100, and 102 K there is the clear indication for another secondary peak at much higher frequencies. Its position does not seem change as temperature is lowered from 106 down to 98 K, while ν_α decreases by several orders of magnitude. Hence, it cannot be the JG relaxation. This feature in the spectrum is unique to 4MH and not found in the other methylated hydrocarbons. Its origin is uncertain because of the lack of experimental data at higher frequencies.⁴⁴

According to the CM, the ratio ν_{JG}/ν_α depends on n for a constant ν_α . Hence the frequency dispersion of 4-methylheptane should be similar to other glass-formers having values of n comparable to 0.28 of 4-methylheptane, even though they have widely different chemical structures. This similarity is demonstrated by the isothermal dielectric loss data of glycerol^{6,9,40} in the inset of Fig. 5, showing the KWW fit with $n=0.29$ (solid line) and the locations of the calculated ν_0 (vertical arrows). Glycerol is just one of many other examples that can be chosen to demonstrate the similarity of their spectra to 4-methylheptane. They include propylene carbonate ($n=0.27$),^{6,9} cresolphthalein-dimethylether ($n=0.25$),⁴⁵ and N-methyl- ϵ -caprolactam ($n=0.24$).⁶ Hence, the dynamics of the JG and the α relaxation in 4-methylheptane conform to the general rule on their relation derived from the CM for glass formers having smaller n .

IV. DISCUSSION AND CONCLUSION

The methylated alkanes studied are derived by attaching one or more methyl groups individually on various carbons on the alkane chain. Other than the attached methyl groups, there is no subgroup the motion of which can be identified with the weak secondary relaxation observed in the methylated alkanes. However, from other experimental works it is known that the rotational motion of the attached methyl group is fast, and decoupled from or not merged with the α relaxation. On the other hand, the observed secondary relaxation is slow, tracks with the α relaxation in the equilibrium liquid state, and shows signs of merging with the α relaxation (see changes of the isothermal spectra in Figs. 1 and 4 on increasing temperature). Hence the attached methyl group or groups cannot be responsible for the observed slow secondary relaxation. Just as in rigid molecular glass formers (chlorobenzene and toluene) or polymer without side groups (1,2 or 1,4 polybutadiene), the existence of the secondary relaxation found in the methylated alkanes is intriguing. There is the possibility that these secondary relaxations, which involves the motion of the entire molecule, may play a

fundamental role in generating the cooperative α -relaxation through many-molecule dynamics. That is the reason why these secondary relaxations have to be distinguished from the trivial ones of intramolecular origin by classifying them as the Johari-Goldstein relaxations. Criteria based on properties have been suggested to distinguish the JG relaxations among secondary relaxations.⁶ In this work we use one of these criteria that comes from the coupling model. This criterion, Eq. (4), says that the JG relaxation time is in approximate agreement with the primitive relaxation time calculated entirely from the parameters of the α relaxation. The criterion have been shown to work previously for the JG relaxations in many glass-formers, and here also in the methylated alkanes. This is the principal result of this work.

Parameters characterizing the α relaxation of the methylated alkanes have been given in Ref. 22 and here in the previous section. The parameters include the Kohlrausch exponent $(1-n)$ and the steepness (fragility) index⁴⁶ m

$$m = \left. \frac{d \log_{10}(\tau_\alpha/s)}{d(T_{\text{ref}}/T)} \right|_{T=T_{\text{ref}}}, \quad (9)$$

where T_{ref} is an arbitrarily chosen temperature at which $\tau_\alpha(T_{\text{ref}})$ is equal to a specified long time.⁴⁶ The standard practice is to take $\tau_\alpha(T_{\text{ref}})=100$ as done in Ref. 22 for the methylated alkanes. Data of many glass-formers indicate that m anticorrelates⁴⁶ with $(1-n)$, or correlates with n . However, there are exceptions.⁴⁷ The notable ones are propylene carbonate ($n=0.27$, $m=91$) and cresolphthalein-dimethylether ($n=0.25$, $m=72.5$).⁴⁵ They have large m but small n when compared with either glycerol^{47,48} ($n=0.29$, $m=53$) or OTP ($n=0.50$, $m=81$).^{39,48-50} The deviation from the correlations by some glass formers could be rationalized by saying that the exceptions have unusual physical or chemical structures, although this is by no means a satisfactory explanation. This rationalization fails here because deviations from the correlation are found in the family of methylated alkanes having similar chemical structures. The most conspicuous case comes from a comparison of 4-methylheptane ($m=46$, $T_g=98.8$ K, $n=0.28$) with 3-methylheptane ($m=47$, $T_g=97.4$ K, $n=0.45$). They have about the same m and T_g , but their n parameters are so different. They belong to the same chemical family except they have different architectures, i.e., 4-methylheptane is a symmetric molecule but not 3-methylheptane. This is a good example of the breakdown of the correlation between m and n that cannot be easily rationalized. On the other hand, 2,4,6-methylheptane ($m=63$, $T_g=122.7$ K, $n=0.44$) is symmetric as 4-methylheptane, but it does not show an exception to the correlation because it has largest m as well as n . According to the CM, the dispersion of the α relaxation or n is determined mainly by the many-molecules dynamics engendered by intermolecular interactions or coupling. The dependence of molecular mobility on temperature, volume V , and entropy S has already entered²⁶ into the primitive relaxation time τ_0 , as evidenced by the non-Arrhenius temperature dependence,^{9,50} the dependence on pressure P of the JG relaxation time in the equilibrium liquid state,⁷ and other properties⁴ The many-molecule dynamics magnify the de-

pendences of $\tau_0(T, P, V, S)$ via Eq. (2) and give rise to the observed stronger dependences²⁶ of $\tau_\alpha(T, P, V, S)$. Since the T_g -scaled temperature dependence of τ_α (i.e., m) is determined by $\tau_0(T, P, V, S)$ and n in addition, it is not surprising that the correlation between m and n can breakdown in some glass formers.

Closely related in chemical composition to the methylated alkanes are the self-assembled alkyl nanodomains with size of 2 nm formed by alkyl groups of different monomeric units in higher members of poly(n -alkyl acrylates) and poly(n -alkyl methacrylates).²³ A polyethylene-like glass transition occurs within the alkyl nanodomains. The larger alkyl nanodomains with size of about 2 nm formed in poly(n -octal acrylates) and poly(n -octal methacrylates) are now compared with the methylated alkanes in properties. One property is the steepness index m . Although the standard practice is to take $\tau_\alpha(T_{\text{ref}})=100$ s, but for cases in which τ_α has not been actually determined for such long times and is only estimated by extrapolation using the VFT law [Eq. (5)], a more prudent choice of T_{ref} is a shorter $\tau_\alpha(T_{\text{ref}})$. This practice was done for the polyethylenelike glass transition in the alkyl nanodomains²³ with the choice of $\tau_\alpha(T_{\text{ref}})=10^{-1}$ s. The values of m are equal to 29 and 33 for the alkyl nanodomains in poly(n -octal acrylates) and poly(n -octal methacrylates), respectively. The coupling parameter n in the KWW exponent $(1-n)$ was deduced²⁴ to have the value of 0.35 and 0.33 for the alkyl nanodomains in poly(n -octal acrylates) and poly(n -octal methacrylates) respectively. From the VFT fits to τ_α [Eq. (5)] of the methylated alkanes, the values of m can be

calculated from the formula, $m = (-1-A) + T_0(-1-A)^2/B$, for the same choice of $\tau_\alpha(T_{\text{ref}})=10^{-1}$ s. The values of m is 48 for 2,4,6-trimethylheptane, 36 for 3-methylpentane, 39 for 2,3-dimethylpentane, 37 for 3-methylheptane, and 36 for 4-methylheptane. Recalling the n values of the methylated alkanes from the previous section, the combination of the two parameters (m, n) are (36, 0.39) for 3-methylpentane, (39, 0.39) for 2,3-dimethylpentane, and (36, 0.28) for 4-methylheptane. These are not far from the combinations (29, 0.35) for the alkyl nanodomains in poly(n -octal acrylates) and (33, 0.33) in poly(n -octal methacrylates), respectively. The comparable m and n values of some of these methylated alkanes and the alkyl nanodomains are not unexpected because their chemical structures are closely related. The similarity goes further in that there is evidence of the presence of an unresolved Johari-Goldstein secondary relaxation in the alkyl nanodomains.²⁴ In both cases, the JG relaxation time is in approximate agreement with the calculate primitive relaxation time.

ACKNOWLEDGMENTS

This work was supported by the Office of Naval Research. I thank Don J. Plazek for a careful reading of the manuscript and the suggestion of designating the materials studied as methylated alkanes instead of branched alkanes. I also thank Ranko Richert for generously supplying his published data digitally, otherwise this work would not be possible.

-
- ¹S. Hensel-Bielowka and M. Paluch, Phys. Rev. Lett. **89**, 025704 (2002).
- ²S. Hensel-Bielowka, J. Ziolo, M. Paluch, and C. M. Roland, J. Chem. Phys. **117**, 2317 (2002).
- ³S. Pawlus, M. Paluch, M. Sekula, K. L. Ngai, S. J. Rzoska, and J. Ziolo, Phys. Rev. E **68**, 021503 (2003).
- ⁴K. L. Ngai and M. Paluch, J. Chem. Phys. **120**, 857 (2004).
- ⁵K. L. Ngai, J. Chem. Phys. **109**, 6982 (1998).
- ⁶K. L. Ngai, J. Phys.: Condens. Matter **15**, S1107 (2003).
- ⁷D. Prevosto, S. Capaccioli, M. Lucchesi, P. A. Rolla, and K. L. Ngai, J. Chem. Phys. **120**, 4808 (2004).
- ⁸K. L. Ngai and S. Capaccioli, Phys. Rev. E **69**, 031501 (2004).
- ⁹K. L. Ngai, P. Lunkenheimer, C. León, U. Schneider, R. Brand, and A. Loidl, J. Chem. Phys. **115**, 1405 (2001).
- ¹⁰K. Y. Tsang, K. L. Ngai, Phys. Rev. E **54**, R3067 (1997).
- ¹¹K. L. Ngai and K. Y. Tsang, Phys. Rev. E **60**, 4511 (1999).
- ¹²K. L. Ngai, IEEE Trans. Dielectr. Electr. Insul. **8**, 329 (2001).
- ¹³K. L. Ngai and R. W. Rendell, in *Supercooled Liquids, Advances and Novel Applications*, edited by J. T. Fourkas, D. Kivelson, U. Mohanty, and K. Nelson, Vol. 676 of ACS Symposium Series, (American Chemical Society, Washington, DC, 1997), Chaps. 4, 45.
- ¹⁴G. P. Johari and M. Goldstein, J. Chem. Phys. **53**, 2372 (1970).
- ¹⁵G. P. Johari, J. Chem. Phys. **58**, 1766 (1973).
- ¹⁶G. P. Johari, Ann. N.Y. Acad. Sci. **279**, 117 (1976).
- ¹⁷G. P. Johari, J. Non-Cryst. Solids **307-310**, 317 (2002).
- ¹⁸C. Mai, S. Etienne, J. Perez, and G. P. Johari, Philos. Mag. B **50**, 657 (1985).
- ¹⁹K. Pathmanathan and G. P. Johari, J. Phys. C **18**, 6535 (1985).
- ²⁰R. Brand, P. Lunkenheimer, and A. Loidl, J. Chem. Phys. **116**, 10386 (2002).
- ²¹J. M. Pelletier, B. Van de Moortele, and I. R. Lu, in *Science of Metastable and Nanocrystalline Alloys and Structures, Properties and Modelling*, edited by A. R. Dineson *et al.* (Riso National Laboratory, Roskilde, Denmark, 2001), p. 359.
- ²²S. Shahriari, A. Mandanici, L.-M. Wang, and R. Richert, J. Chem. Phys. **121**, 8960 (2004).
- ²³M. Beiner and H. Huth, Nat. Mater. **2**, 595 (2003).
- ²⁴K. L. Ngai and M. Beiner, Macromolecules **37**, 8123 (2004).
- ²⁵K. L. Ngai, R. W. Rendell, in *Relaxation in Complex Systems and Related Topics*, edited by I. A. Campbell and C. Giovannella (Plenum Press, New York, 1990), pp. 309-316.
- ²⁶K. L. Ngai, in *Slow Dynamics in Complex Systems: Third International Symposium on Slow Dynamics in Complex Systems*, edited by Michio Tokuyama and Irwin Oppenheim, AIP Conf. Proc. No. 708 (AIP, Melville, 2004), p. 515.
- ²⁷E. R. Weeks, J. C. Crocker, A. Levitt, A. Schofield, and D. A. Weitz, Science **287**, 627 (2000).
- ²⁸R. Richert, Europhys. Lett. **54**, 767 (2001); K. Duvvuri and R. Richert, J. Chem. Phys. **118**, 1356 (2003).
- ²⁹R. Böhmer, G. Hinze, T. Jörg, F. Qui, and H. Sillescu, J. Phys.: Condens. Matter **12**, A383 (2000).

- ³⁰M. Vogel and E. Rössler, *J. Chem. Phys.* **114**, 5802 (2000).
- ³¹M. Vogel, C. Tschirwitz, G. Schneider, C. Koplin, P. Medick, and E. Rössler, *J. Non-Cryst. Solids* **307-310**, 326 (2002).
- ³²R. Böhmer, G. Diezemann, G. Hinze, and E. Rössler, *Prog. Nucl. Magn. Reson. Spectrosc.* **39**, 191 (2001).
- ³³H. Sillescu, R. Böhmer, G. Diezemann, and G. Hinze, *J. Non-Cryst. Solids* **307-310**, 16 (2002).
- ³⁴Ranko Richert, Kalyan Duvvuri, and Lien-Thi Duong, *J. Chem. Phys.* **118**, 1828 (2003).
- ³⁵K. Schmidt-Rohr and H. W. Spiess, *Phys. Rev. Lett.* **66**, 3020 (1991).
- ³⁶S. A. Reinsberg, X. H. Qiu, M. Wilhem, H. W. Spiess, and M. D. Ediger, *J. Chem. Phys.* **114**, 7299 (2001).
- ³⁷S. A. Reinsberg, A. Heuer, B. Doliwa, H. Zimmermann, H. W. Spiess, *J. Non-Cryst. Solids* **307-310**, 208 (2002).
- ³⁸K. L. Ngai and C. M. Roland, *Polymer* **43**, 567 (2002).
- ³⁹H. Wagner and R. Richert, *J. Phys. Chem. B* **103**, 4071 (1999).
- ⁴⁰U. Schneider, R. Brand, P. Lunkenheimer, and A. Loidl, *Phys. Rev. Lett.* **84**, 5560 (2000).
- ⁴¹See Fig. 2 of R. Casalini, M. Paluch, and C. M. Roland, *Phys. Rev. E* **67**, 031505 (2003); Figure 6(f) of K. L. Ngai, *J. Phys.: Condens. Matter* **15**, S1107 (2003).
- ⁴²See Fig. 1 of O. E. Kalinovskaya and J. K. Vij, *J. Chem. Phys.* **111**, 10979 (1999).
- ⁴³K. L. Ngai, J. Habasaki, C. Leon, and A. Rivera, *Z. Phys. Chem. (Munich)* **219**, 47 (2005).
- ⁴⁴R. Richert (private communication).
- ⁴⁵M. Paluch, K. L. Ngai, and S. Hensel-Bielowka, *J. Chem. Phys.* **114**, 10872 (2001).
- ⁴⁶R. Böhmer, K. L. Ngai, C. A. Angell, and D. J. Plazek, *J. Chem. Phys.* **99**, 4201 (1993).
- ⁴⁷K. L. Ngai, *J. Non-Cryst. Solids* **275**, 7 (2000).
- ⁴⁸C. León and K. L. Ngai, *J. Phys. Chem.* **103**, 4045 (1999).
- ⁴⁹K. L. Ngai, L.-R. Bao, A. F. Yee and C. Soles, *Phys. Rev. Lett.* **87**, 215901 (2001).
- ⁵⁰M. Paluch, C. M. Roland, S. Pawlus, J. Ziolo, and K. L. Ngai, *Phys. Rev. Lett.* **91**, 115701 (2003).